

Electron Inertial Effects on Alfvén Modes at Magnetic X-points

K. G. McClements¹, A. Thyagaraja¹, P. J. Knight¹, N. Ben Ayed², L. Fletcher³

¹EURATOM/UKAEA Fusion Association, Culham Science Centre, Abingdon, UK

²H.H. Wills Physics Laboratory, University of Bristol, Bristol, UK

³Department of Physics & Astronomy, University of Glasgow, Glasgow, UK

1 Introduction

Magnetic X-points exist close to the boundary of divertor tokamaks and, in tokamaks generally, are produced by reconnection of magnetic field lines resulting from MHD instabilities. In order to interpret realistic non-linear calculations of turbulence and spectral transfer processes in X-point configurations, it is important to understand both the linear mode spectrum and the temporal behaviour of perturbations in such configurations. We present solutions of the eigenvalue problem and the initial value problem for an idealised X-point with zero equilibrium current, taking into account resistivity and electron inertia.

2 Eigenvalue Spectrum: $B_z=0$

With resistive and electron inertial terms included in Ohm's law, the linearised cold plasma induction and momentum equations for a system whose equilibrium is described by a field $\mathbf{B}_E=B_0(\hat{y}x + x\hat{y})/R_0$, $B_z=0$, zero flow and uniform density can be written in the form [1]

$$\frac{\partial}{\partial t} \left[\psi - \frac{\delta_e^2}{r} \frac{\partial}{\partial r} \left(r \frac{\partial \psi}{\partial r} \right) \right] = vr + \frac{1}{Sr} \frac{\partial}{\partial r} \left(r \frac{\partial \psi}{\partial r} \right) \quad \frac{\partial v}{\partial t} = \frac{\partial}{\partial r} \left(r \frac{\partial \psi}{\partial r} \right) \quad (1)$$

where $\mathbf{B} = \nabla \times (\psi \hat{z})$, v is perturbed flow speed, r is radial distance in units of the system size R_0 , t is time in Alfvén units, $\delta_e = c/(\omega_{pe} R_0)$ is collisionless skin depth, and S is Lundquist number. As shown in Fig 1, the eigenvalue spectrum of this system has two distinct continua, corresponding to zero and finite real mode frequencies ω : in the latter case, the intrinsic damping rate in Alfvén units is $1/(2S\delta_e^2)$ for all ω [2]. A finite number of discrete modes can also exist, depending on the values of S and δ_e , and are present in the limit of zero skin depth [3]. However, when the resistive scale length $1/S^{1/2}$ is smaller than the skin depth, as is generally the case in tokamaks, the spectrum is purely continuous.

3 Solution of Initial Value Problem: $B_z=0$

As described in [1], we have also solved numerically the initial value problem represented by the pair of equations (1) for a current-free two-dimensional X-point with an azimuthally

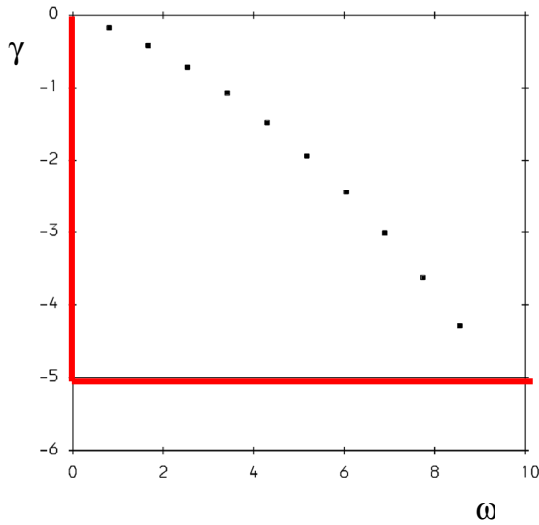


Figure 1 X-point eigenvalue spectrum for $B_z=0$, Lundquist number $S=10^3$ and collisionless skin depth $\delta_e=0.01$. Frequency ω and growth rate γ are in Alfvén units. Discrete modes are indicated by squares, & solid red lines at $\gamma=-5$ & $\omega=0$ indicate finite and zero frequency continua respectively. All eigenmodes of the system are damped, since the equilibrium configuration is potential. The boundary conditions $\partial\psi/\partial r=0$ at $r=0$ and $r=1$ were used in both the spectral analysis and the initial value calculations.

symmetric field perturbation and $v=0$ at $t=0$ (for $B_z=0$ the system remains azimuthally symmetric at all times). Because the Alfvén speed decreases with r , non-potential magnetic field energy and ion flow energy are focused towards the X-point. When $1/S^{1/2} > \delta_e$ total field energy \mathcal{E}_f is initially observed to reach equipartition with total flow energy \mathcal{E}_{ki} , in accordance with ideal MHD, and is then dissipated extremely rapidly, on an Alfvénic timescale that is essentially independent of resistivity (Fig 2a). The field energy and flow energy then decay on a longer timescale and exhibit oscillatory behaviour, reflecting the

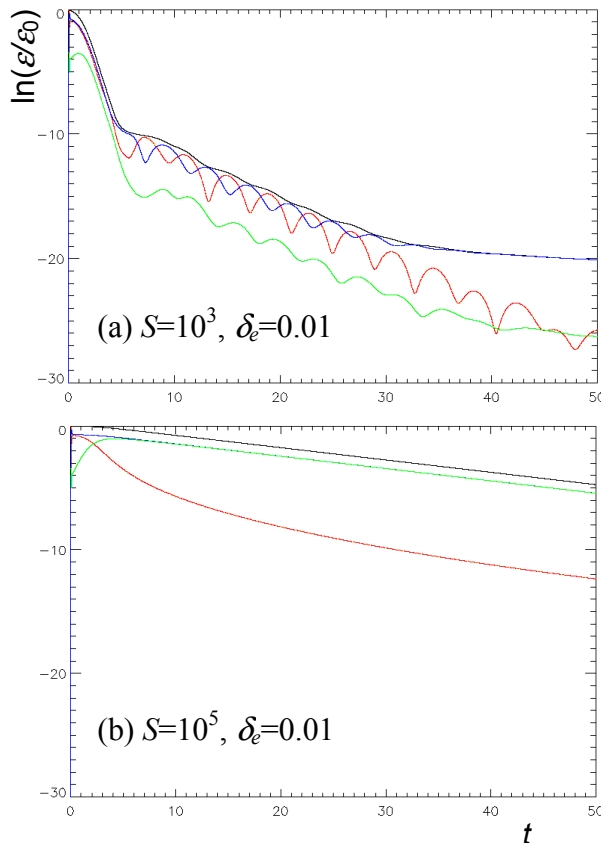


Figure 2 Time evolution of normalised total energy \mathcal{E} (black curves), perturbed magnetic field energy (red), ion kinetic energy (blue) and electron kinetic energy (green) for perturbed X-point configurations with resistive scale length (a) greater than and (b) less than the collisionless skin depth. The initial state of the system is $v=0$ and $\psi \sim -\exp[-100(\ln r)^2]$, i.e. a localised disturbance far from the X-point itself. Oscillations of the energy components in (a) are due to the presence of the discrete normal modes shown in Fig 1. For the parameters in (b) the spectrum is purely continuous and the field energy decays much more rapidly than the kinetic energy due to phase mixing. Similar results are obtained when the initial field perturbation extends over the entire solution domain.

existence of discrete normal modes. On a yet longer timescale, the oscillations disappear and $\epsilon_{ki} \gg \epsilon_f$: this can be attributed to the zero frequency continuum [1]. When $1/S^{1/2} < \delta_e$, the system again evolves initially according to ideal MHD (Fig 2b). Due to phase mixing associated with the finite frequency continuum, the field energy then decays on an Alfvénic timescale, while the kinetic energy (which is equally partitioned between ions and electrons in this case) is dissipated on the electron collision timescale. The oscillatory decay in the energy observed in the resistive limit is absent, but filamentary structures appear in the field and velocity profiles, again due to phase mixing (cf. [4]), suggesting the possibility of particle acceleration in oppositely-directed current channels [1].

4 Solution of Initial Value Problem: $B_z \neq 0$

The model has been extended to include the effects of a strong longitudinal (toroidal) magnetic field. The linearised three-dimensional induction and momentum equations are solved using CENTORI, a fully toroidal two-fluid plasma turbulence code. Results obtained in the ideal limit show that the presence of a toroidal field slows down but does not prevent the focusing of field and kinetic energy towards the X-point observed in the two-dimensional model (Fig 3). However, field perturbations that are initially azimuthally symmetric no

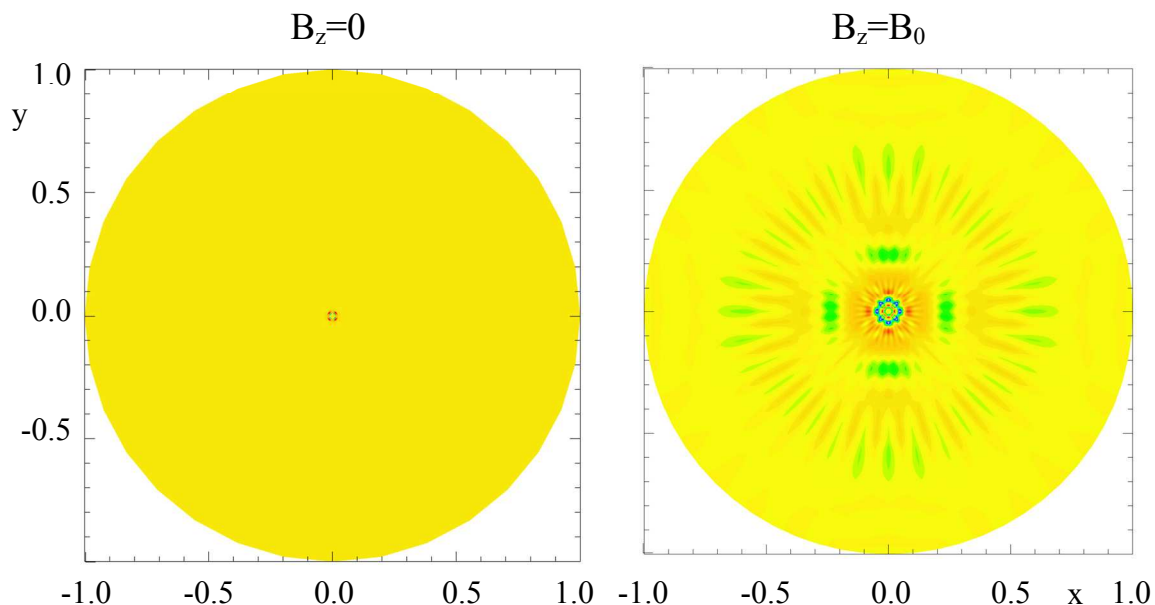


Figure 3 CENTORI computations of perturbed azimuthal magnetic field B_θ after five Alfvén times for $S \rightarrow \infty$, $\delta_e = 0$ and $B_z=0$ (left), $B_z=B_0$ (right). Initially $B_\theta \sim \sin(\pi r)$, $v=0$. In the case of $B_z=B_0$ field energy has cascaded into Alfvénic modes with short azimuthal wavelengths.

longer remain so as the system evolves. When $B_z=B_0$ oscillations are superposed on the energy components as they approach equipartition (Fig 4b); when $B_z \gg B_0$ the oscillations disappear (Fig 4c) and the system evolution is similar to that of the $B_z=0$ case (Fig 4a). In all cases equipartition is reached on the azimuthal Alfvén timescale.

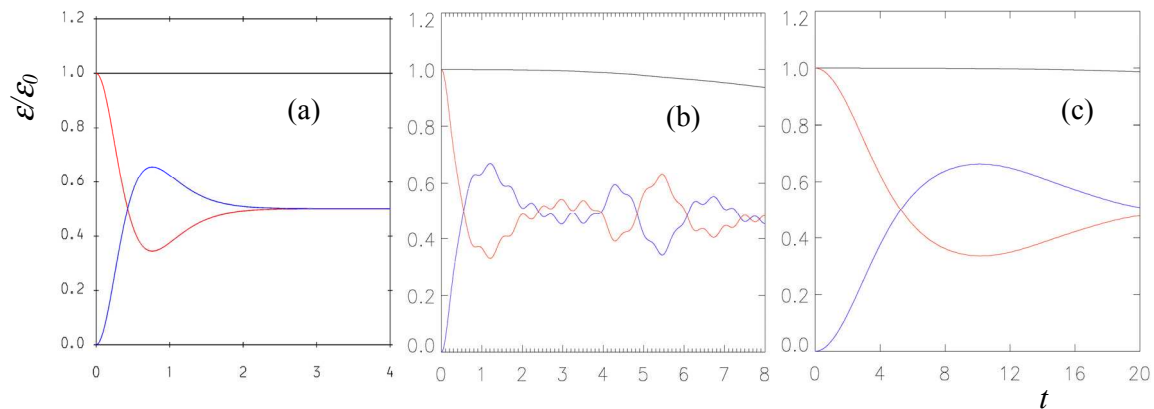


Figure 4 Evolution of normalised total energy $\varepsilon/\varepsilon_0$ (black), perturbed B-field energy (red) and ion kinetic energy (blue) for (a) $B_z=0$, (b) $B_z=B_0$ and (c) $B_z=10B_0$. Time t is in units of R_0/c_A where c_A is Alfvén speed at $R=R_0$. The curves in (a) were obtained analytically, while those in (b) and (c) were computed using CENTORI. The deviation of $\varepsilon/\varepsilon_0$ from unity in (b) and (c) is purely numerical.

5 Conclusions

When resistivity and electron inertia are taken into account, the eigenmode spectrum of a current-free cold plasma magnetic X-point with zero longitudinal field (B_z) can be shown to have discrete and continuous components; two distinct continua exist, with zero and finite real frequencies ω . When $B_z=0$ and the collisionless skin depth is greater than the resistive length, phase mixing due to the finite ω continuum causes filamentation of field and velocity profiles and the transfer of field energy to kinetic energy on the Alfvén timescale. Finite B_z breaks the azimuthal symmetry of the $B_z=0$ case, but in the ideal limit the field and kinetic energy reach equipartition on the azimuthal Alfvén timescale irrespective of B_z . Possible applications of this work include tearing modes and edge localised modes (ELMs) in tokamaks, and short timescale energy release in solar flares [1].

Acknowledgements This work was funded jointly by the United Kingdom Engineering and Physical Sciences Research Council and by EURATOM.

- [1] K G McClements et al., *Astrophys. Journal*, in press (2004).
- [2] K G McClements, A Thyagaraja, *Plasma Phys. Control. Fusion* **46** (2004) 39.
- [3] I J D Craig, A N McClymont, *Astrophys. Journal* **371** (1991) L41.
- [4] F Porcelli et al., *Plasma Phys. Control. Fusion* **44** (2002) A389.